Open access • Journal Article • DOI:10.1063/1.2828111

Full-field imaging of nonclassical acoustic nonlinearity — Source link

Bart Sarens, Georgios Kalogiannakis, Christ Glorieux, Danny Van Hemelrijck

Institutions: Katholieke Universiteit Leuven

Published on: 27 Dec 2007 - Applied Physics Letters (American Institute of Physics)

Topics: Shearography and Nonlinear acoustics

Full-field imaging of nonclassical acoustic nonlinearity

Bart Sarens, Georgios Kalogiannakis,[a] and Christ Glorieux[b]
Laboratorium voor Akoestiek en Thermische Fysica, Departement Fysica en Sterrenkunde, Katholieke Universiteit Leuven, Celestijnenlaan 200D, B-3001 Heverlee, Belgium

Danny Van Hemelrijck
Department of Mechanics of Materials and Constructions, Vrije Universiteit Brussel, Pleinlaan 2, B-1050 Brussels, Belgium

(Received 3 May 2007; accepted 3 December 2007; published online 27 December 2007)

The feasibility of full field shearographic detection of nonclassical acoustic nonlinearity is investigated. Traditional frequency analysis of the sinusoidally excited sample, as used in scanning techniques, turns out to be not practical due to the inherent optical detection nonlinearity of the shearography system itself. An alternative method, based on determining the asymmetry between shearographic images stroboscopically obtained for positive and negative displacements, is proposed. This approach allows us to easily and rapidly detect the tension-compression asymmetry which typically arises where nonbounded contact interface defects are present. © *2007 American Institute of Physics*. [DOI: 10.1063/1.2828111]

Nonlinear acoustic methods have become increasingly popular in recent years in the field of nondestructive testing (NDT) due to their enhanced sensitivity and especially their "defect selective" behavior. In practice, cracks and delaminations are often "closed" (nonbonded contact interfaces) so that traditional linear techniques fail to detect them due to lack of acoustic mismatch. In nonlinear acoustics, the instantaneous change of the geometrical features of the defect, induced by a high amplitude elastic stimulus, leads to defect "clapping." Essentially, the defect area behaves differently when the local stress rises above a certain threshold value (defect opened) as when the local stress is lower than this threshold (defect closed). In the case of harmonic excitation, this effect can be observed by detecting higher harmonics in the displacement signal at the defect location. This nonclassical acoustic nonlinearity is directly associated with the presence of a defect and allows us to detect nonbonded closed defects with high contrast.[1–11]

Several nonlinear acoustic techniques have emerged during the past decade in an effort to exploit this potential. The detection scheme typically made use of ultrasonic transducers[8–10] or a scanning laser Doppler vibrometer.[11] Though a significant breakthrough was achieved to demonstrate the power of nonlinear acoustics in terms of defect detection and identification, the scanning approach has the drawback of having to compromise between optimum spatial resolution and signal-to-noise ratio on one hand, and speed of operation on the other hand. In this work, we remediate this dilemma by upgrading the approach to a full-field shearographic imaging implementation.

Shearography is an optical technique[12,13] based on the speckle effect and is widely used in NDT applications.[14–16] In order to visualize periodic phenomena at frequencies higher than the frame rate of the charge coupled device camera, we have stroboscopically illuminated the sample surface (using a modulated probe laser) at particular temporal phases of the vibration cycle. The used experimental setup basically consists of a shearography system (ISI-Systems®), synchronized with the excitation source (Fig. 1). The sample under investigation (Fig. 2) is a unidirectional carbon/epoxy composite plate $[0°]_{16}$ (Hexcel-Fibredux 920CX-TS-5-42), which has an area of 300×300 mm^2 and a total thickness of 2 mm. This type of material was selected as it is typically used in advanced applications where the timely detection of defects is crucial. An artificial delamination was created by locally placing a thin circular Teflon film (20 mm diameter and 10 μm thickness) between the second and third ply below the surface under investigation (Fig. 2). In addition, the plate was impacted above the delamination (3.5 J) with a ball of 25 mm diameter. Since the plates undergo a curing procedure under high temperature and uniform pressure, the resulting surface is smooth and there is no externally visible indication of the delamination. In order to implement the acoustic excitation, a 35 mm diameter piezoelectric transducer (0.55 mm thickness) was attached to the plate (Fig. 2).

In shearography, the intensity at a particular point of the image corresponds to the superposition of the light scattered from two adjacent points in the original object that are slightly sheared (by use of a beam splitter and adjustable mirror) with respect to each other. For simplicity, let the separation of these points be δx parallel to the x axis. The optical phase difference $\Delta\phi$ between two slightly sheared

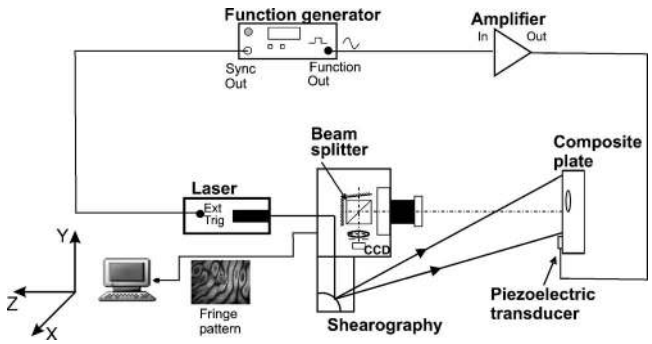

FIG. 1. Schematic layout of the experimental system and the object under investigation.

[a]Electronic mail: georgios_kalogiannakis@yahoo.com and georgios.kalogiannakis@yahoo.com.
[b]Electronic mail: christ.glorieux@fys.kuleuven.be.

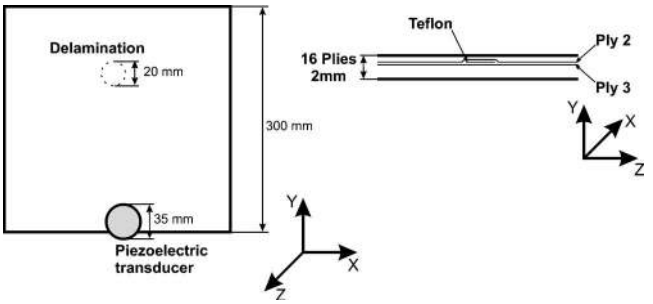

FIG. 2. Layout of the sample structure. An artificial delamination was created by introducing a thin circular Teflon film (indicated by the dashed circle) between the second and third ply of a composite plate. A piezoelectric transducer was used to generate a standing wave pattern.

interfering scattered laser beams at a pixel location may be approximated as follows:

$$\Delta\phi(x,y,t) = \frac{2\pi\delta x}{\lambda}(1+\cos\theta)\left(\frac{\partial d_z(x,y,t)}{\partial x}\right) \equiv kf(t), \quad (1)$$

where θ is the illumination angle with respect to the viewing direction, d_z is the surface out-of-plane displacement, and $k \equiv 2\pi\delta x(1+\cos\theta)/\lambda$. It should be stressed that the in-plane components of the surface displacement are considered too small to be relevant. The sensitivity of the fringes can be therefore adjusted by varying the orientation of the adjusting mirror and thereby the shearing distance δx. The resulting interference intensity $I(x,y,t)$ can be readily evaluated by

$$I(x,y,t) = \frac{I_{\max}+I_{\min}}{2} + \frac{I_{\max}-I_{\min}}{2}\cos[\phi_0(x,y) + \Delta\phi(x,y,t)], \quad (2)$$

where $I_{\min}$ and $I_{\max}$ are, respectively, the intensities for fully destructive and fully constructive interference and $\phi_0(x,y)$ is the optical phase pattern for the sample in reference conditions (e.g., for the sample in rest, or for an arbitrarily chosen point in the vibration cycle). For the sake of contrast formation, one is evaluating the relative temporal intensity variations, which are obtained by subtracting the reference (in our case, the specklegram at rest) from each subsequent pattern. As a result, speckle correlation fringes are formed. For large optical phase variations due to displacements of the order of and larger than one optical wavelength, the intensity images depend on $f(t)$ in a very nonlinear way [see Eq. (2)]. This makes a traditional frequency analysis not feasible because the harmonics induced by the nonlinearity of the optical detection system are large, thus masking weak harmonics due to the nonlinear elastic response of a defect in the sample. In theory, phase shifting techniques allow us to determine the absolute optical phase and thereby the absolute surface slope and displacement image for every stroboscopic temporal phase, thus eliminating the optical detection nonlinearity typical for raw intensity images. Although a wide range of techniques is available to filter, demodulate, and integrate intensity images in such an approach, it turns out to be very difficult to obtain a fast and reliable result in practice.

Here, we propose a simpler and more straightforward technique to detect local defect-induced asymmetric behavior[7] (while in compression the delamination behaves like intact material, in tension the stiffness is much lower as the delamination is allowed to open). Speckle correlation fringes were obtained by subtracting subsequent specklegrams from the reference image at rest. By subtracting these intensity correlation images at maximum positive and maximum negative displacement excursions of the sample, one can also detect nonclassical acoustic nonlinearity. Indeed, in the case of linear (or classical nonlinear) behavior, the relative temporal intensity images at maximum and minimum displacements (or otherwise the two antisymmetric positions in the cycle where we obtain the highest fringe density) are identical, thus resulting in a zero intensity image. Only at locations undergoing defect-induced nonclassical nonlinear behavior, which is intrinsically connected with tension-compression asymmetry,[7] these images will be different and the subtracted image will no longer be zero.

In practice, the temporal phase of a local vibration has a nontrivial relation with the phase of the excitation source. As a result, when performing a subtraction at a given stroboscopic temporal phase in the sinusoidal excitation cycle, the difference image is not only related to the asymmetry induced by the defect but it also depends on the map of the displacement pattern and resulting interferogram for the chosen phase. Therefore, the asymmetry map for a given phase is convolved by a distorting pattern of peaks and nulls of the interferogram.

In order to counter this, the following approach was taken: a series of interferometric images was recorded with different temporal phases with respect to the excitation signal (e.g., images at 0°, 10°, 20°,…,350°). For each case, the corresponding images with 180° phase difference were subtracted (0°–180°, 10°–190°,…). Then, the sum of the absolute values of these different images was taken. In this way, the asymmetry was averaged over the entire displacement cycle of the sample and peaks and nulls of the stroboscopic interferograms were smeared out. As a result, the obtained image clearly indicates the defect location, with strongly reduced interferometric effects.

The result of an experimental implementation of this approach can be seen in Fig. 3. Here, a sinusoidal excitation signal was applied on the piezoelectric transducer. As a result, a standing wave pattern arose in the plate. The excitation frequency was chosen so that an antinode of the standing wave pattern occurred at the (known) position of the artificial defect. For cases where the position of the defect is not known in advance, the experiment must be repeated for a range of frequencies to increase the probability for all regions of the plate to be efficiently excited. The plate was slightly bent toward the viewing direction so that the defect remains definitely closed at rest. The images in Fig. 3(a) were taken for relatively low excitation amplitude (50 V peak to peak). The internal stress gradients were too small to open the artificial delamination. As a result, the elastic behavior remained linear so that the resulting specklegrams at for instance 90° and 270° are identical and their difference is almost zero. Figure 3(b) shows the specklegrams obtained for high excitation amplitude (200 V peak to peak). For that case, the internal stress gradients were large enough to open the delamination so that the sample started to show a nonlinear elastic response at that location. As a result, the fringe patterns at 90° and 270° locally differ and the subtracted image shows the location of the defect. Also after performing the described asymmetry averaging over the vibration cycle (difference images were recorded for 36 phases and their

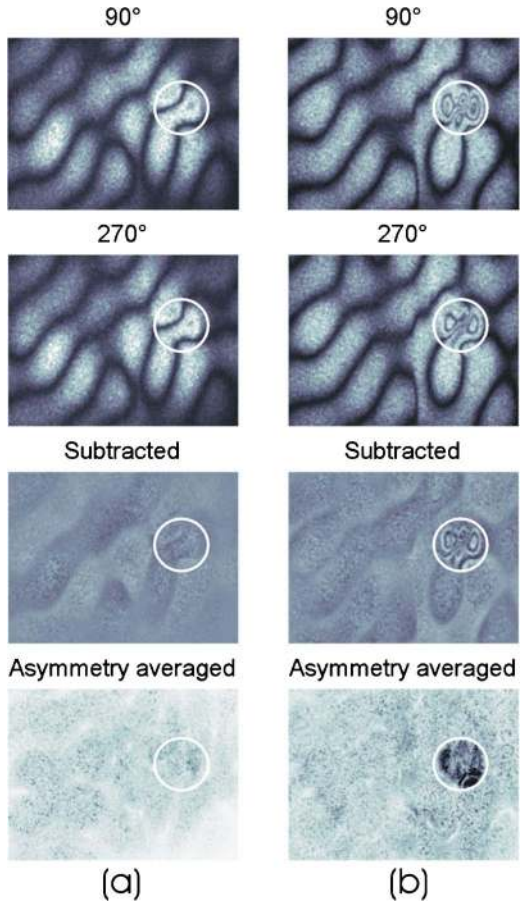

FIG. 3. Stroboscopically obtained shearographic images of speckle correlation fringes and difference images obtained for a sinusoidal excitation signal applied on the piezoelectric transducer ($f=18.3$ kHz). (a) Images obtained with a low excitation amplitude. The first two rows show the intensity images at 90° and 270° temporal phase (with regard to the excitation signal), respectively. The third row shows their difference. The fourth row shows the improved result after asymmetry averaging over the displacement cycle. (b) Images obtained with the same approach, but the excitation amplitude was increased by a factor of 4. The shearing distance was different for the two experiments to allow for optimal fringe visibility. The gray scale was kept the same for the subtracted and asymmetry averaged images. To guide the eye of the reader, the defect is indicated by a circle.

absolute value was averaged), the defect location is revealed in an enhanced way, with virtually no interferometric effects remaining. The shape of the fringes in the subtracted image is influenced by the properties of the defect as well as by optical parameters of the setup, rendering their interpretation not straightforward. Therefore, the specific properties of the defect and its exact behavior are difficult to determine and describe in this short communication and will be the subject of future work. However, for purposes of NDT, the method shows to be very feasible and robust for defect detection. Interestingly, the nonlinear behavior is selectively provoked right above the defect, allowing for defect localization with high lateral spatial resolution.

In conclusion, while scanning nonlinear detection techniques traditionally relied on a temporal frequency analysis, requiring time intensive point wise spectral analysis, the newly proposed method allows a fast and robust full field detection of nonclassical nonlinearity with good lateral spatial resolution at the price of more complexity in the relation between the images and the acoustical displacement, but keeping the important advantage to visualize defects that would remain invisible with low amplitude linear acoustic/mechanic techniques.

The authors express their gratitude to the Institute for the Promotion of Innovation through Science and Technology in Flanders (IWT-Vlaanderen) and the Research Council of Katholieke Universiteit Leuven (Project No. GOA/2007/06/TBA) for funding this research.

[1] O. Buck, W. L. Morris, and J. M. Richardson, Appl. Phys. Lett. **33**, 371 (1978).
[2] O. Buck and W. L. Morris, J. Acoust. Soc. Am. **64**, 33 (1978).
[3] K. Van den Abeele and M. A. Breazeale, J. Acoust. Soc. Am. **41**, 1112 (1996).
[4] K. Van Den Abeele, P. A. Johnson, R. A. Guyer, and K. R. McCall, J. Acoust. Soc. Am. **101**, 1885 (1997).
[5] S. Hirsekorn, Ultrasonics **39**, 57 (2001).
[6] S. Hirsekorn and P. Delsanto, Appl. Phys. Lett. **84**, 1413 (2004).
[7] I. Y. Solodov, N. Krohn, and G. Busse, Ultrasonics **40**, 621 (2002).
[8] V. Zaitsev, V. Gusev, and B. Castagnede, Phys. Rev. Lett. **89**, 105502 (2002).
[9] I. Y. Solodov, J. Wackerl, K. Pfleiderer, and G. Busse, Appl. Phys. Lett. **84**, 5386 (2004).
[10] V. Tournat, V. Zaitsev, V. Gusev, V. Nazarov, P. Béquin, and B. Castagnède, Phys. Rev. Lett. **92**, 085502 (2004).
[11] N. Krohn, R. Stoessel, and G. Busse, Ultrasonics **40**, 633 (2002).
[12] J. A. Leendertz and J. N. Butters, J. Phys. E **6**, 1107 (1973).
[13] Y. Y. Hung and C. E. Taylor, Exp. Mech. **14**, 281 (1974).
[14] L. X. Yang, W. Steinchen, G. Kupfer, P. Mackel, and F. Vossing, Opt. Lasers Eng. **30**, 199 (1998).
[15] J. W. Newman, Mater. Eval. **636**, 746 (2005).
[16] L. X. Yang, Mater. Eval. **64**, 703 (2006).